IEEE Access
Multidisciplinary | Rapid Review | Open Access Journal

Received February 22, 2019, accepted March 3, 2019, date of publication March 20, 2019, date of current version April 11, 2019.

Digital Object Identifier 10.1109/ACCESS.2019.2906461

A Time-Integral Crack Propagation Model Considering Thickness Effect

JUNZHOU HUO[1], ZHANGE ZHANG[1], ZHICHAO MENG[1], LIN XUE[1], GUOPENG JIA[1], AND JING CHEN[2]

[1]School of Mechanical Engineering, Dalian University of Technology, Dalian 116024, China
[2]School of Navigation and Shipbuilding Engineering, Dalian Ocean University, Dalian 116023, China

Corresponding authors: Lin Xue (linxue@dlut.edu.cn) and Zhange Zhang (zhange@mail.dlut.edu.cn)

This work was supported in part by the National Key R&D Program of China under Grant 2018YFB1306701, in part by the National Natural Science Foundation of China under Grant 51875076, and in part by the NSFC-Liaoning United Key Fund under Grant U1708255.

ABSTRACT The crack propagation mechanism of thick plates is difficult to describe accurately, and thus, it is difficult to predict the lifetimes of thick plate structural cracks in extreme construction environments. In this paper, a theoretical model of the time-integrated crack propagation that accounts for the thickness effect is established. The constraint factor is introduced to characterize the thickness effect of crack propagation, and the constraint factor formula was obtained by fitting the experimental results. The results of the fatigue crack growth tests and the crack propagation theoretical predictions for Q345D specimens showed the time-integrated crack propagation model predicts the crack propagation more accurately in the initial stage and during the stable expansion stage of crack propagation. These results have guiding significance for the fatigue life prediction of equipment with thick plate structural features.

INDEX TERMS Thick plate, crack propagation, crack closure, fatigue test, time integration method.

I. INTRODUCTION

Fatigue failure is one of the most important factors for the working efficiency of engineering equipment, and it is affected by material, by loading, by the thickness and by the environment. The fatigue of metal is divided into two stages: crack initiation and crack propagation. For material, the fatigue life is equal to the sum of crack initiation life and crack extension life, and the crack initiation life is greater than the crack extension life. For thick plate components of engineering equipment, such as tunnel boring machine cutters, large excavator buckets, and large engine casing parts, it is generally believed that the fatigue life is equal to the crack extension life; that is, the crack initiation life is not factored in [1]. In general, for thick metal components, the crack tip has a complex three-dimensional stress state; that is, not a plane stress state or a plane strain state. Furthermore, plates of different thicknesses have large differences in crack propagation characteristics. Therefore, for the structural characteristics of thick plates, it is imperative to study the crack propagation mechanism and accurately predict the fatigue lives.

The associate editor coordinating the review of this manuscript and approving it for publication was Poki Chen.

There has been considerable research on crack propagation. The Paris formula is the most common classical crack propagation model. Since this formula was presented, researchers have considered the fracture threshold K_{th}, the stress ratio R, the crack closure effect, the crack tip stress relaxation, and other factors, and have repeatedly revised the Paris formula. Meanwhile, new models have also been proposed. Typical models include the Mc Evily model [2], Walker formula [3], Forman formula [4], Newman model [5], and Elber formula [6]. Mohanty *et al.* [7], [8] proposed an index model for crack propagation under banner loading and overload conditions, which can accurately predict the second and third stages of fatigue crack propagation. Jones *et al.* [9] proposed a fatigue life prediction method based on the Dugdale model. Lu and Liu [10] proposed a two-dimensional surface crack propagation model under a plane stress state, which avoids the problem of load loss and loading sequence in the cyclic counting method when dealing with variable amplitude loads. Chen *et al.* [11] proposed a theoretical model for fatigue crack growth caused by nine parameters by modifying the McEvily model and explained overload hysteresis and low-load acceleration under overload conditions to effectively predict the crack propagation behavior. Shi *et al.* [12] proposed a type I fatigue crack

growth rate model using the strain energy failure mechanism in the plastic zone of tip stress crack propagation and verified the model using multi-axis metal material fatigue crack propagation data to predict safety. Bao *et al.* [13] introduced two energy-based predictive models to predict the fatigue crack growth behaviors of traditional compact tension (CT) and small-sized C-shaped inside edge-notched tension (CIET) specimens with different thicknesses and load ratios. Different values of the effective stress ratio U were employed in the theoretical fatigue crack growth models to correct for the effect of crack closure. Correia *et al.* [14] used the normalized fatigue crack growth model proposed by Castillo *et al.* to propose a general fatigue life prediction method based on structural details using fracture mechanics. The cyclic J-integral range was used instead of the stress intensity factor range as a reference parameter to extend the CCS model. Irwin [15] first proposed the use of constraint factors to describe the effect of thickness on crack propagation and used the constraint factor to correct the crack growth rate. Subsequently, Newman *et al.* [16], [17], Newman [18] obtained the relationship between the crack growth rate and the stress intensity factor of an aluminum alloy under different stress ratios based on a test method. The constraint factor of the 2.3 mm aluminum alloy sample was reversed, and the constraint factor and crack opening ratio were compared. J.J. Schubbe [19] and others performed experimental studies of the effect of plate thickness on the crack growth rate of 7050-T7451 aluminum alloy thick plates. Huo *et al.* [20] and Sun *et al.* [21], [22] modified a small-timescale crack-growth model to predict the crack-growth lifetime of a Tunnel Boring Machine(TBM) cutterhead based on the plane stress/strain transition condition. Yu *et al.* [23] studied the plastic closure phenomenon in crack propagation. Based on simulations and a theoretical derivation, the thickness effect in the crack propagation was characterized by the constraint factor. A crack closure model accounting for the thickness influence was proposed. The model also considered the effect of the stress ratio. Shang *et al.* [24] proposed a closed-form theoretical crack tip driving force model using simple expressions for static and fatigue crack propagation along a linear yield strength gradient (YSG) based on the Dugdale criterion. A difference of material-toughening mechanisms between smooth and sharp strength gradients was revealed both theoretically and numerically. Hu *et al.* [25] introduced a cohesive zone model (CZM) that accounted for the fracture process zone (FPZ) located in front of the crack tip using a new singular finite element method to study fatigue crack growth under variable amplitude cyclic loading (VACL). The cohesive stresses were converted to nodal forces of the singular element, and the plastic zone length(PLZ) can be solved numerically by iteration. Yu and Guo [26], [27], Xiang and Guo [28], Guo *et al.* [29] proposed a model for three-dimensional crack propagation under the action of a spectral load based on the influence of the thickness on the plastic zone of the crack tip. The influence of the stress ratio and sample thickness on the crack propagation life was discussed.

In summary, many scholars have made achievements in the research of crack propagation mechanisms and prediction of the crack propagation lifetimes in thick plates. Most of the crack growth rate models are based on solving for stress intensity factors, considering the stress ratio, fracture toughness, and threshold value. These models take the stress cycle as the smallest unit to measure the crack growth. However, the stress of the actual mechanical structure in service is random, and the information will inevitably be lost when the stress time history is transformed. Thus, there is still not a model that can accurately describe the characteristics of crack propagation.

Therefore, by introducing the constraint factor, the plastic deformation zone and crack opening displacement of the crack tip under the plane stress state were modified, and a theoretical model of the time integral crack propagation including the constraint factor is proposed. The constraint factor was fit using the Q345D thick plate fatigue test. Furthermore, the crack propagation lifetime prediction at any timescale for a finite thickness plate with a variable amplitude load in the stable expansion stage was realized.

II. MATERIALS AND METHOD

A. CRACK TIP STRESS FIELD

A fatigue crack that extends across the thickness is called a through-thickness crack. If the fatigue load is only tensile, the leading edge of the crack is perpendicular to the material surface, as shown in Fig 1 (a). For a crack in an infinite plate under tension, the crack tip can be regarded as an elliptical hole with zero height, and the approximate solution can be obtained in polar coordinates for the limit stress at a point close to the crack tip. In theory, the stress tends to be infinite at the crack tip. In fact, due to the excessive stress at the crack tip, a small plastic zone appears at the crack tip, where the infinite peak stress is flattened. As shown in Fig 1 (c), r_p is the size of the plastic zone. Due to the shrinkage of the plastic zone, the plastic zone at the crack front is much smaller than the thickness of the thick plate with a penetrating crack, and the lateral shrinkage at the crack front will be limited. At this stress level, the free surface near the two sides of the thick plate is in a plane stress state, and the region from the plane strain state to the plane stress state is transited. The width is r_p, and the thick plate is in the plane stress state, as shown in Fig 1 (b).

Assuming elastic behavior, the stress at a point near the crack tip is expressed as follows:

$$\begin{aligned}
\sigma_x &= \frac{K_I}{\sqrt{2\pi r}} \cos\frac{\theta}{2}\left(1 - \sin\frac{\theta}{2}\sin\frac{3\theta}{2}\right) \\
\sigma_y &= \frac{K_I}{\sqrt{2\pi r}} \cos\frac{\theta}{2}\left(1 + \sin\frac{\theta}{2}\sin\frac{3\theta}{2}\right) \\
\tau_{xy} &= \frac{K_I}{\sqrt{2\pi r}} \sin\frac{\theta}{2}\cos\frac{\theta}{2}\cos\frac{3\theta}{2},
\end{aligned} \tag{1}$$

where σ_x is the x-direction stress, σ_y is the y-direction stress, τ_{xy} is the shear stress of the x-y plane, K_I is the crack stress intensity factor, r is the distance from a point near the crack

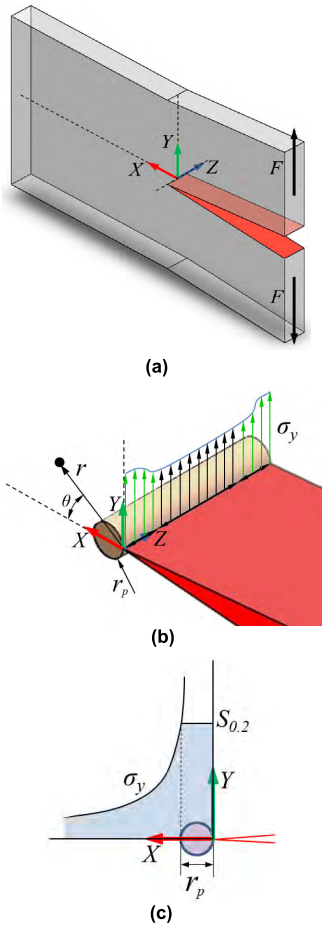

FIGURE 1. Three-dimensional crack front stress field of thick plate. (a) Type I crack. (b) Stress field of crack front. (c) Stress distribution of crack front.

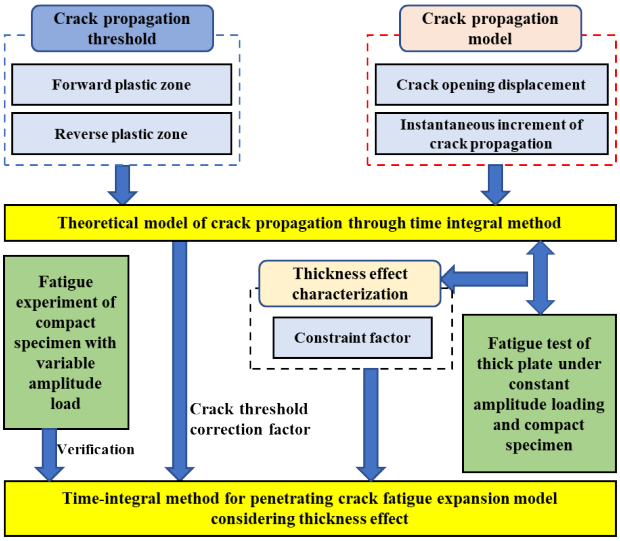

FIGURE 2. Process of time-integrated crack propagation model considering thickness.

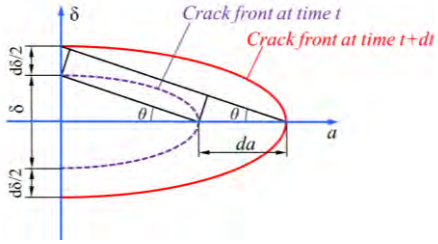

FIGURE 3. Schematic diagram of crack tip expansion [10].

tip to the crack tip, and θ is the plane of the crack propagation plane angle.

B. THEORETICAL PREDICTION MODEL OF TIME INTEGRATION CRACK PROPAGATION

Due to the thick plate effect at the crack front, the plastic flow at the fatigue crack tip is restricted and the stress state at the crack tip changes significantly. The stress state at the crack front exists in a plane stress state, plane strain state, and transition state, and the crack propagation rate also changes. In this paper, a constraint factor is introduced to characterize the effect of the thickness on the crack propagation for a finite thickness component. By modifying the plastic zone at the crack tip and crack opening displacement, a crack propagation model for a thick plate based on time integration is proposed. The flow chart is shown in Fig 2.

It can be seen in Fig 2 that an extended model of the crack was established based on the crack opening displacement and the instantaneous increment of crack propagation. Based on the correction of the forward plastic zone and the reverse plastic zone of the crack front, the threshold of crack propagation was obtained. The simultaneous crack propagation model and the threshold model were used to establish a time-integrated crack propagation model that included the parameters of the constraint factors to be determined. Through the rigid specimen fatigue test of a thick plate with a constant amplitude load, the constraint factor formula was obtained through fitting, and the time-integration method for a penetrating crack fatigue expansion model accounting for the thickness effect was established. Finally, a fatigue test of a compact fatigue specimen with variable amplitude load was applied to validate the model.

1) SURFACE CRACK PROPAGATION MODEL UNDER PLANE STRESS STATE

Based on the time-integrated surface fatigue crack propagation model proposed by Lu the fatigue crack tip expansion at any time and crack length under a normal amplitude load is shown in Fig 3 [10].

The dotted line in Fig 3 indicates the leading edge of the crack at time t, the solid line indicates the crack leading edge at the time $t + dt$, da is the extended length of the crack under a cyclic load, and $d\delta/2$ indicates the crack tip opening displacement (CTOD) under the same cycle load. θ represents the crack opening angle (CTOA), and the crack propagation length and crack opening displacement at times t and t+dt in

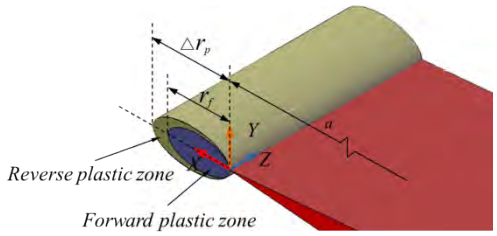

FIGURE 4. Plastic zone of crack tip under constant amplitude loading[10].

a cycle can be obtained based on the geometric relationship in Fig 3:

$$da = \frac{\cot\theta}{2} d\delta. \tag{2}$$

Based on the strip yield model proposed by Liu *et al.* [30], the crack opening displacement during loading and unloading under a plane stress state is:

$$\delta_{reloading} = \delta_{\min,m} + \frac{1}{2\lambda}\left(\sigma - \max\left(\sigma_{\min,m}, \sigma_{ref,m}\right)\right)^2 a, \tag{3}$$

$$\delta_{unloading} = \delta_{\max,m} - \frac{1}{2\lambda}\left(\sigma_{\max,m} - \max\left(\sigma, \sigma_{ref,m}\right)\right)^2 a, \tag{4}$$

$$\lambda = 3\pi/8E\sigma_y, \tag{5}$$

where E is the elastic modulus, σ_y is the yield strength of the material, $\delta_{min,m}$ is the crack opening displacement after *m-th* stress unloading, $\delta_{max,m}$ is the crack opening displacement after *m-th* stress loading cycle, σ represents the nominal stress value of the *(m+1)-th* stress cycle, $\sigma_{min,m}$ is the minimum load of the *m-th* stress cycles, $\sigma_{max,m}$ represents the maximum load of the *m-th* stress cycles, a represents the crack length under the current load cycle, and $\sigma_{ref,m}$ is the fatigue crack growth threshold of the *m-th* stress cycle.

2) THEORETICAL MODEL OF TIME INTEGRAL CR-ACK PROPAGATION PREDICTION UNDER CONSTANT AMPLITUDE LOAD

In the entire process of increasing cyclic stress, the crack tip inevitably produces forward and reverse plastic zones. The crack propagates only when the boundary of the forward plastic zone generated by the new load exceeds the boundary of the reverse plastic zone generated when the previous load is unloaded (as shown in Fig 4), satisfying $r_f = r_p$. The crack growth threshold is calculated by using the well-known formulas of forward and backward plastic zone size. Crack growth will occur only when the stress under load exceeds the crack growth threshold.

The constraint factor α is introduced to consider the influence of the stress state change on the plastic zone of the crack tip due to the thickness effect [31], and the yield stress is corrected to obtain the effective yield stress $\alpha\sigma_y$. The forward plastic zone is calculated using the Irwin formula [32]:

$$r_f = \frac{1}{2\pi}\left(\frac{K^*}{\alpha\sigma_y}\right)^2, \tag{6}$$

$$K^* = \left(\sigma_{ref} - \sigma_{\min}\right)\sqrt{\pi a}, \tag{7}$$

where σ_y is the yield stress of the material.

The backward plastic zone was calculated using the method proposed by McClung [33]:

$$\Delta r_p = \frac{1}{2\pi}\left(\frac{\Delta K_{eff}}{2\alpha\sigma_y + (\sigma_c - \sigma_{\min})}\right)^2, \tag{8}$$

where σ_c is the crack closure stress, $\sigma_c = \sigma_{ref}$; ΔK_{eff} is the effective stress intensity factor amplitude, $\Delta K_{eff} = \sigma_{max}$-$\sigma$, σ_{ref} is the crack propagation threshold, σ_{min} is the minimum stress in the cyclic load, and σ_{max} is the maximum stress in the load cycle.

The threshold of crack propagation is

$$\sigma_{ref} = \frac{-\left(3\alpha\sigma_y - 2R\sigma_{\max}\right)}{2} + \frac{\sqrt{\left(3\alpha\sigma_y - 2R\sigma_{\max}\right)^2 - 4\sigma_{\max}\left[R^2\sigma_{\max} - (2R+1)\,\alpha\sigma_y\right]}}{2}, \tag{9}$$

where R is the stress ratio, $R = \sigma_{min}/\sigma_{max}$, and σ_{max} is the maximum stress in the load cycle.

In the process of cyclic loading, differentiating the crack opening displacement δ of the loading section yields

$$d\delta_{reloading} = \frac{\lambda}{a} a\left(\sigma - \sigma_{ref,m}\right) d\sigma + \frac{\lambda}{2a}\left(\sigma - \sigma_{ref,m}\right)^2 da. \tag{10}$$

The crack opening displacement formula is obtained by differentiating with respect to time t on both sides:

$$\frac{1}{a}\frac{da}{dt} = \frac{2\lambda\left(\sigma - \sigma_{ref,m}\right)\cot\theta}{2 - \lambda\left(\sigma - \sigma_{ref,m}\right)^2\cot\theta}\frac{d\sigma}{dt}. \tag{11}$$

It can be seen from the above formula that after obtaining the stress time history of the crack tip, the time is integrated to obtain the amount of crack propagation. When the stress in a cycle changes from σ_{min} to σ_{max}, the crack length extends from a_0 to $a_0 + \Delta a$ under the constant amplitude load. Due to the crack closure effect, the crack propagates only when the stress σ is larger than the crack propagation threshold $\sigma_{ref,m}$ in the current cycle. For the above integral, the crack propagation length under a constant amplitude load can be obtained:

$$\Delta a = \frac{da}{dN} = \frac{a_0 \cdot C \cdot \lambda \cdot \left(\sigma_{\max} - \sigma_{ref,m}\right)^2}{2 - C \cdot \lambda \cdot \left(\sigma_{\max} - \sigma_{ref,m}\right)^2}, \tag{12}$$

$$C = cot\theta/2. \tag{13}$$

3) TIME INTEGRAL CRACK PROPAGATION PREDICTION MODEL UNDER VARIABLE AMPLITUDE LOAD

The crack leading edge under a variable amplitude load is shown in Fig 5.

During the cyclic load loading process, the variable amplitude load begins when the crack propagation length is a_{ol}, and the reverse plastic zone generated is $\Delta r_{p,ol}$ when the cyclic load is unloaded. For the crack propagation length a,

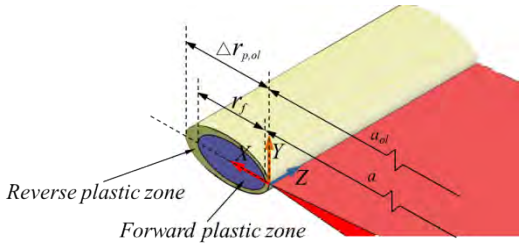

FIGURE 5. Plastic zone of crack tip under variable amplitude load [10].

the forward plastic zone size under the current load is r_f. The threshold condition for crack propagation when the variable amplitude load occurs is:

$$a_{ol} + \Delta r_{p,ol} = a + r_f \tag{14}$$

The constraint factor α is introduced to consider the influence of the stress state change under the thickness effect on the plastic zone of the crack tip. The effective yield stress is $\alpha\sigma_y$.

$$r_f = \frac{1}{2\pi}\left(\frac{\Delta K}{a\sigma_y}\right)^2, \tag{15}$$

$$\Delta r_{p,ol} = \frac{1}{2\pi}\left(\frac{\left(\sigma_{\max,ol} - \sigma_{ref}\right)\sqrt{\pi a_{ol}}}{2a\sigma_y + \left(\sigma_{ref} - \sigma_{\min,ol}\right)}\right)^2. \tag{16}$$

The corresponding crack propagation threshold is:

$$\sigma_{ref} = \frac{-\left(3a\sigma_y - 2R\sigma_{\max}\right)}{2} + \frac{\sqrt{\left(3a\sigma_y - 2R\sigma_{\max}\right)^2 - 4\sigma_{\max}\left[R^2\sigma_{\max} - (2R+1)\,a\sigma_y\right]}}{2} \tag{17}$$

Considering the crack blunting caused by the variable amplitude load, the threshold stress correction factor η is introduced to correct the crack propagation threshold when the crack propagation threshold is solved:

$$\sigma_{eqref} = \eta\sigma_{ref}, \tag{18}$$

where η is the threshold correction factor, and the values of the threshold correction factors for different materials are different, generally between 1.3 and 1.6. σ_{eqref} is the modified equivalent crack propagation threshold,

In the process of cyclic loading, differentiating the crack opening displacement δ of the loading section can be obtained:

$$d\delta_{reloading} = \frac{\lambda}{\alpha}a\left(\sigma - \sigma_{eqref,m}\right)d\sigma + \frac{\lambda}{2\alpha}\left(\sigma - \sigma_{eqref,m}\right)^2 da. \tag{19}$$

The crack opening displacement formula is obtained by differentiating with respect to time t on both sides:

$$\frac{\alpha da}{C\lambda a} = \frac{2\left(\sigma - \sigma_{eqref,m}\right)d\sigma}{2 - C\left(\lambda/\alpha\right)\left(\sigma - \sigma_{eqref,m}\right)^2}. \tag{20}$$

When the internal stress of a cycle changes from σ_{min} to σ_{max}, the crack length is extended from a_0 to $a_0 + \Delta a$ under the variable amplitude load. Due to the existence of the crack closure effect, the crack propagates only when the stress σ is larger than the crack propagation effective threshold $\sigma_{eqref,m}$ in the current cycle. For the above formula, the crack propagation length under arbitrary load can be obtained:

$$\Delta a = \frac{da}{dN} = \frac{a_0 \cdot C \cdot (\lambda/\alpha) \cdot \left(\sigma_{\max} - \sigma_{eqref,m}\right)^2}{2 - C \cdot (\lambda/\alpha) \cdot \left(\sigma_{\max} - \sigma_{eqref,m}\right)^2}. \tag{21}$$

Based on the constraint factor and the threshold correction factor, a crack propagation length calculation model for thick plate structures under arbitrary loads is established considering the stress ratio and crack closure effect.

C. CONSTRAINT FACTOR MODEL BASED ON FATIGUE TEST

First, the undetermined coefficient was used to modify the constraint factor model using the constraint factor calculation model proposed by Yu and Guo [27]. Second, the Q345D compact tensile specimen was used to carry out the fatigue crack growth test, and the experimental results were brought into the established time integral crack propagation prediction model to obtain the constraint factor of the corresponding thickness. Finally, the constraint factor was included in the model, and the final constraint factor model was obtained.

1) CONSTRAINT FACTOR MODEL

According to the study by Yu and Guo [27], the size of the constraint factor is related to the thickness of the plate and the size of the plastic zone:

$$a = g\left(r_p/B\right), \tag{22}$$

$$r_p = \frac{\pi}{8}\left(\frac{K_{\max}}{\sigma_y}\right)^2, \tag{23}$$

$$g\left(x\right) = \frac{1 + a(\sqrt{x} + 2x^2)}{1 - 2\nu + b(\sqrt{x} + 2x^2)}, \tag{24}$$

where B is the thickness of the sample and r_p is the plastic zone size when the crack begins to expand stably. The plastic zone size r_p is modeled using the Dugdale-Barenblatt model. K_{max} is the maximum stress intensity factor under alternating stress, σ_y is the yield stress of the material, and a and b are coefficients to be determined.

2) FATIGUE EXPANSION EXPERIMENT UNDER CONSTANT AMPLITUDE LOAD

a: EXPERIMENTAL SAMPLE

The compact tensile fatigue specimen developed following the GBT6398-2000 standard [34] was used for this experiment.

b: TEST EQUIPMENT AND INSTRUMENTS

Our research group established a set of fatigue test benches, as shown in Fig 6 below. These were mainly composed of a

base, gantry, actuator, hydraulic station, controller, computer, cooling station, and fixture. The base was fixed to the ground, and the gantry and the base were fixed by bolts. The end of the actuator was mounted to the gantry, and the actuator end and sample were fixed. The hydraulic station provided a load for the actuator to achieve fatigue test loading. The cooling station cooled the loading system using hydraulic oil. The clamp was fixed to the base by bolts.

c: FATIGUE EXPANSION TEST

Artificial cutting was performed by wire cutting to facilitate fatigue crack initiation. Subsequently, 2 mm fatigue cracks were prefabricated by a high amplitude cyclic load, and the fatigue tests were initiated. In the crack propagation experiment, the crack propagation of the compact tensile specimen was measured in real time by means of an industrial camera and a Vernier caliper, and the number of cycles was recorded.

3) DETERMINATION OF CONSTRAINT FACTOR PARAMETERS

First, the relationship between the nominal dynamic stress and crack length a_0 on the crack propagation path of the compact tensile specimens was established using a quasi-static method. Second, the dynamic stress and experimental crack growth rate were substituted into the time-integral crack growth prediction model, and the constraint factor of the corresponding thickness was calculated. Third, the dynamic stress and the experimental crack propagation rate were substituted into the established time integral crack propagation model, and the constraint factor of the corresponding plate thickness was calculated. Finally, the experimentally calculated constraint factor was used in the constraint factor model, and the relevant parameters of the constraint factor model were obtained to form the final constraint factor formula.

a: DYNAMIC STRESS SOLUTION

By solving for the unit stress generated by the unit load at different positions and multiplying the result by the actual load time history, the dynamic stress of the component can be obtained. Finally, the solved dynamic stress components were superimposed to solve the final dynamic stress:

$$\sigma_{(t)} = \sum p_{(t)} \frac{\sigma}{F}, \tag{25}$$

where $P_{(t)}$ is the external load of the fatigue test.

Using the finite element analysis method, a unit static force F was applied to the two semi-circular holes of the sample model. The length of the crack incision was increased and the nominal tensile stress σ at the midpoint of the different crack lengths was extracted. Subsequently, the expression of the unit tensile stress σ/F and the fatigue crack length a_0 of the compact tensile specimen was obtained and multiplied by the load spectrum function to obtain the dynamic stress function.

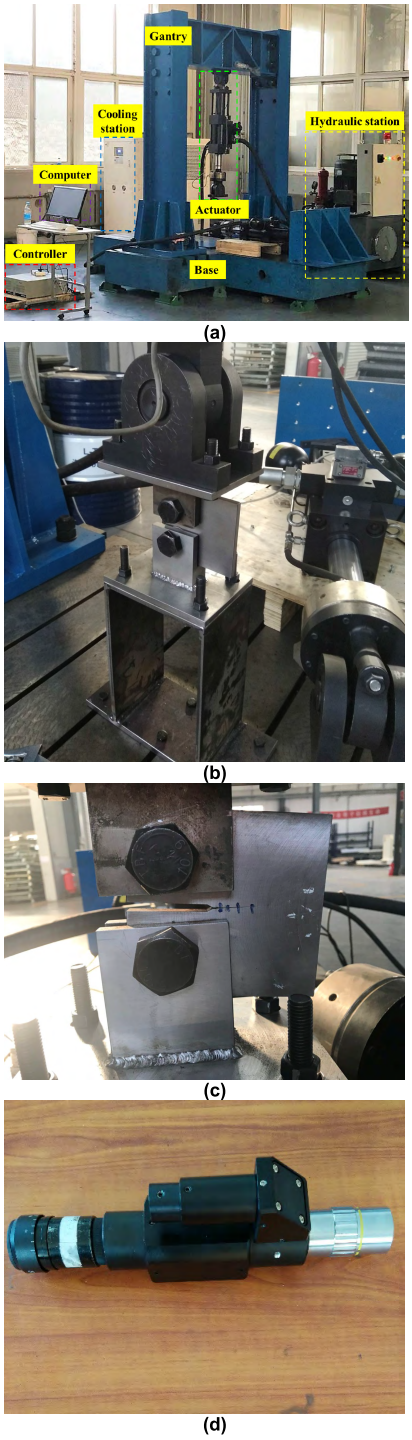

FIGURE 6. Fatigue test and crack measuring instrument. (a) Fatigue test bench. (b) Fixture. (c) Compact tensile test specimen. (d) Industrial camera.

b: CONSTRAINT FACTOR

Fatigue crack propagation results of samples with different thicknesses obtained by experiment. The experimental results were brought into the established time integral crack propagation model, and the constraint factors of the corresponding plate thickness were obtained.

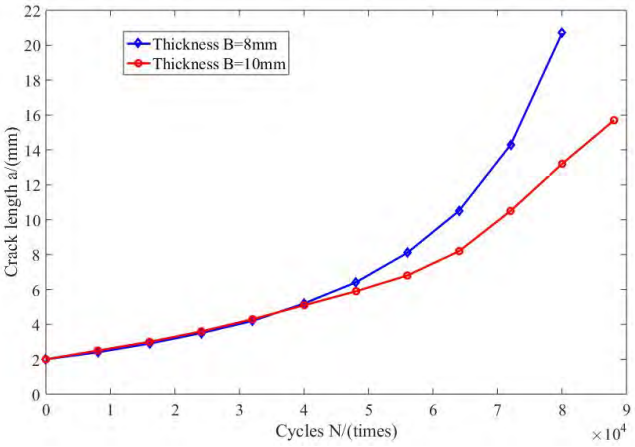

FIGURE 7. Crack growth curves of CT specimens with two thickness under constant amplitude loading.

TABLE 1. Dimensional parameters of compact tensile specimens.

Material	W/mm	B/mm	an/mm	h/mm	N
Q345D	100	8	30	4	3
Q345D	100	10	30	4	3

c: CONSTRAINT FACTOR MODEL PARAMETER DETERMINATION

Based on the constraint factors of the samples with different thicknesses, the regression constraint factor formula can be used to find the undetermined parameters in the formula, and the final constraint factor calculation model is obtained.

D. CRACK PROPAGATION EXPERIMENT OF C(T) SPECIMEN UNDER CONSTANT AMPLITUDE LOAD

An artificial cut was introduced using a wire cutting to facilitate fatigue crack initiation. A prefabricated 2 mm initial fatigue crack was exposed to a variable amplitude load with $P_{max} = 30$ kN and $P_{min} = 8$ kN. Subsequently, the load was transferred to the maximum load for the experiment in two stages, and the fatigue test was initiated. The load spectrum function was as follows:

$$P_{(t)} = 13 + 7\sin(20\pi t). \tag{26}$$

The constant crack propagation experiments were carried out in 2 groups with a total of 6 compact samples. The samples and parameters are shown in Fig 7(a) and Table 1, in which there are three 8 mm thick specimens and three 10 mm thick specimens. The sample material was Q345D. The width of all the samples was 100 mm. The initial crack depth was 30 mm, and the slit width was 4 mm. For the Q345D material, the crack opening angle was 11.5°, and the threshold correction factor was 1.6 [20].

Real-time measurements of the crack propagation in compact tensile specimens were obtained using industrial cameras and Vernier calipers in the constant-load crack propagation experiments. The loading was stopped, but the load was not removed when making the crack length measurements. At the time of measurement, the crack length of two surfaces of the specimen were measured. The average of the two measurements were used as the crack extension length at this time, and the number of cycles was recorded.

After obtaining the crack propagation results of the two sets of samples, the average crack propagation results of the three samples with the same thicknesses were averaged. Respectively, the crack propagation length a and the number of cycles N of a compact tensile specimens with thicknesses of 8 and 10 mm were obtained, and the crack propagation rate was solved by the secant method GBT6398-2000.

E. CRACK PROPAGATION TEST OF C(T) SPECIMEN UNDER VARIABLE AMPLITUDE LOAD

An artificial cut was introduced using wire cutting to facilitate fatigue crack initiation. The prefabricated 2 mm initial fatigue cracks were exposed to a variable amplitude load with $P_{max} = 30$ kN and $P_{min} = 8$ kN. Subsequently, the load was transferred to the maximum load for the experiment in two stages, after which the fatigue test was initiated. The load $P_{(t)}$ consisted of two low-high load functions, as shown in the following equation:

$$P_{(t)} = \begin{cases} 14 + 6\sin(20\pi t) \\ (0 + N \cdot T_0 \le t \le 10000T + N \cdot T_0) \\ 16 + 8\sin(20\pi t) \\ (10000T + N \cdot T_0 \le t \le 15000T + N \cdot T_0), \end{cases} \tag{27}$$

where T represents the duty cycle, $T = 0.1$ s; T_0 is the entire load cycle period, $T_0 = 15000$ T; and N is the number of cycles, $N = 0, 1, 2$.

The constant crack propagation experiment was carried out in 3 groups with 9 compact samples. There were three 10 mm thick samples, three 12 mm thick samples, and three 14 mm thick samples. The sample material was Q345D, the widths of all the samples were 100 mm, the initial crack depth was 30 mm, and the slit width was 4 mm. For the Q345D material, the crack opening angle was 11.5°, and the threshold correction factor was 1.6.

Real-time measurements of the crack propagation in the compact tensile specimens were obtained using industrial cameras and Vernier calipers in the variable amplitude load crack propagation experiments. The loading was stopped, but the load was not removed when performing the crack length measurements. During the measurement, the crack lengths of the two surfaces of the sample were measured. The average of the two was used as the crack extension length at this time, and the number of cycles was recorded.

After obtaining the crack propagation results of the three sets of samples, the crack propagation results of the three samples with the same thicknesses were averaged. The crack propagation length a and the number of cycles N of the compact tensile specimens with thicknesses of 10, 12, and 14 mm were obtained, and the crack propagation rate was solved by the secant method GBT6398-2000.

TABLE 2. Constraint factor for CT specimens with thicknesses of 8 and 10 mm.

Material	Thickness B/mm	Initial crack length a0/mm	Constraint factor α
Q345D	8	2	1.08
Q345D	10	2	1.20

III. RESULTS

A. EXPERIMENTAL RESULTS OF CRACK PROPAGATION OF C(T) SPECIMEN UNDER CONSTANT AMPLITUDE LOAD

(1) Experimental results of crack propagation of C(T) specimens with constant amplitude load

The fatigue crack growth rates for the compact tensile specimens were measured. The crack propagation length a and the number of cycles N of the compact tensile specimens with thicknesses of 8 and 10 mm are shown in Fig 7.

As can be seen from Fig 7, the two types of compact tensile specimens exhibited the same overall expansion trend. The crack growth rate of the sample increased with the increase of the fatigue crack growth length. When the number of cycles reached 80,000, the cracks of the specimens with 8 mm thicknesses grew to 20.6 mm, and those of the 10 mm thickness specimens grew to 13.2 mm. The crack growth rate of the C(T) specimens with different thicknesses were significantly different.

(2) Constraint factor model calculation

The stresses of crack-tip under unit load at different crack lengths were obtained by finite element analysis. The unit tension stress σ/F of a compact tension specimen was fit by the stresses and crack lengths in least square method:

$$\sigma/F = 0.309a_0 + 9.9424. \tag{28}$$

Based on the nominal dynamic stress formula, the nominal dynamic stress of the crack growth in the compact tension specimen was obtained:

$$\sigma_{(t)} = 4.017a_0 + 129.2512 + (2.163a_0 + 69.5968)\sin 20\pi t. \tag{29}$$

The experimental results were brought into the established time-integrated crack propagation model, and the constraint factors for the two sample thicknesses are shown in Table 2.

The obtained constraint factor was inserted into the constraint factor model to obtain the undetermined coefficient $a = 0.0831$ and $b = 0.1111$. The final constraint factor calculation model is:

$$g(x) = \frac{1 + 0.0831(\sqrt{x} + 2x^2)}{1 - 2\nu + 0.1111(\sqrt{x} + 2x^2)} \tag{30}$$

B. EXPERIMENTAL RESULTS OF CRACK PROPAGATION OF C(T) SPECIMEN UNDER VARIABLE AMPLITUDE LOAD

The crack propagation length and number of cycles of three thickness specimens under variable amplitude load were obtained by experimental methods. The results of the three groups of samples with the same thicknesses were averaged to obtain the crack propagation length and the number of cycles. The experimental curves for the fatigue expansion of the CT specimens with three thicknesses and variable amplitude load cracks are shown in Fig 8.

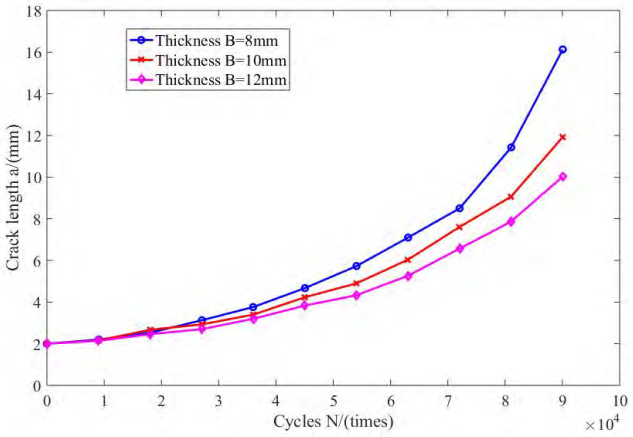

FIGURE 8. Crack growth curves of CT specimens with three thickness under variable amplitude loading.

C. PREDICTION OF CRACK PROPAGATION OF CT SPECIMENS BASED ON TIME INTEGRAL

Calculation of the dynamic stress at the tip of fatigue crack was performed by a quasi-static method. The relationship between the crack propagation dynamic stress and the crack propagation length of a sample having a thickness of 10 mm is as follows:

$$\sigma_{(t)} = \begin{cases} 4.326a_0 + 139.1936 + (1.854a_0 + 59.6544)\sin(20\pi t) \\ (0 + N \cdot T_0 \le t \le 10000T + N \cdot T_0) \\ 4.944a_0 + 159.0784 + (2.472a_0 + 79.5392)\sin(20\pi t) \\ (10000T + N \cdot T_0 \le t \le 15000T + N \cdot T_0). \end{cases} \tag{31}$$

Among them, a_0 is the crack length. The dynamic stresses of the 12 and 14 mm samples were calculated in the same way.

According to the time-integral crack growth theory model accounting for the thickness effect and the crack growth load boundary, the crack growth laws of specimens with thicknesses of 10, 12, and 14 mm were calculated, as shown in Fig 9.

As can be seen from Fig 9, the fatigue crack propagation trends of three specimens with different thicknesses under variable amplitude loading were generally consistent. Under high amplitude loading, the crack growth rate was higher, and the crack growth rate was lower in the low amplitude loading cycle stage. In the early stage of crack propagation, the error between the theoretical prediction and experimental results was small, and in the later stage of crack propagation,

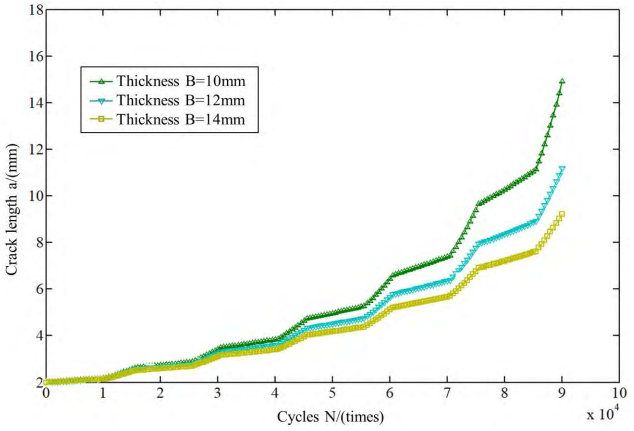

FIGURE 9. Theoretical prediction under variable amplitude loading.

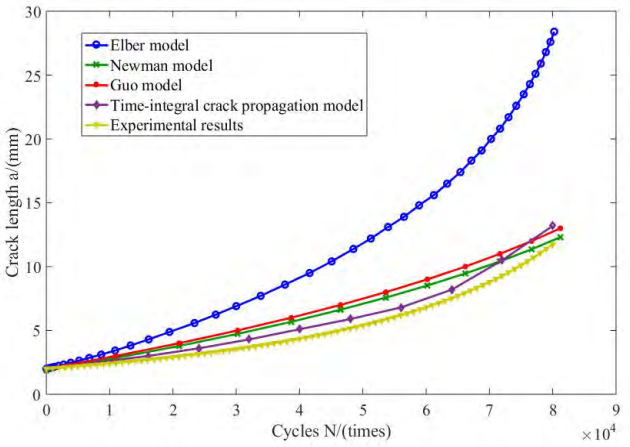

FIGURE 10. Theoretical prediction and experimental results of crack propagation.

the theoretical prediction lagged behind the experimental results.

IV. DISCUSSION

A. COMPARISON OF PREDICTED RESULTS FOR DIFFERENT CRACK GROWTH MODELS UNDER CONSTANT AMPLITUDE LOADING

Based on the Zencrack three-dimensional crack propagation simulation software, the fatigue crack growth simulation of 10 mm C(T) specimen was performed. Based on the simulated stress intensity factor amplitude of the C(T) specimens, the theoretical life of the C(T) specimen crack propagation was solved by combining the Elber, Newman, and Guo models. As a comparison, the time-integral crack growth model that accounts for the thickness effect was used to predict the fatigue life of the 10 mm thick compact tensile specimens. We also performed a fatigue extension test of a compact tensile specimen with a thickness of 10 mm. As evident from the crack life expansion curve, the predicted results of the crack extension model based on the time integral were more accurate than the traditional fracture mechanics model for fatigue life prediction. The specific details are shown in Fig 10.

As shown in Fig 10, the predicted results of the Elber model were quite different from the experimental results. Furthermore, compared to the measured results, the predicted results of the Elber model show that the crack propagation speed was faster and the difference was large. This was because the Elber model accounted for the effect of crack closure. However, the crack opening ratio obtained by fitting was mainly for thin plate specimens, and the effect of thickness on the crack opening ratio was not considered. Therefore, the crack opening ratio calculated was larger, which led to a large deviation of the predicted crack growth from the actual growth. The Newman, Guo, and time integral crack propagation models agreed well with the experimental results. The predicted results of Newman and Guo models were similar, and the predicted results are in good agreement with the experimental results at the initial stage of crack propagation. When the number of load cycles was less than 7×10^4, the predicted expansion speed was greater than the experimental expansion speed. But as the crack propagation length increased, the crack theoretical expansion rate decreased, and when the number of load cycles exceeded 7×10^4, the predicted expansion speed was less than the experimental expansion speed. At the same time, with the increase of the crack propagation length, the theoretical prediction of the crack growth rate and the measured expansion rate was quite different. The time-integrated crack propagation model showed good agreement with the experimental results, and the difference between the extended prediction and the measured result was the smallest. The measured expansion speed was larger than the theoretical prediction expansion speed, but the phase difference was not large. Therefore, the time integral crack propagation model under the constant amplitude load is reasonable.

B. VERIFICATION OF PREDICTION RESULTS OF CRACK PROPAGATION MODEL UNDER VARIABLE AMPLITUDE LOAD

It can be seen from Fig 10 that after 60,000 cycles of cracks, the crack propagation prediction showed good agreement with the test results, and the maximum error was within 0.6 mm. After 60,000 cycles, the theoretical prediction deviated from the test results, and the test results were slightly larger than the time integral theory prediction. The error increased gradually as the crack propagation length increased. After 90,000 cycles, the maximum prediction errors for the samples with thicknesses of 10, 12, and 14 mm were 8.3%, 10.6%, and 8.1%, respectively.

C. IMPACT ANALYSIS OF CRACK PROPAGATION PARAMETERS

(1) Impact analysis of initial crack parameters

The initial crack length was set from 0.1–0.5mm, and the load was the same as that of constant amplitude load test. When the crack lengths of the Q345D specimens with

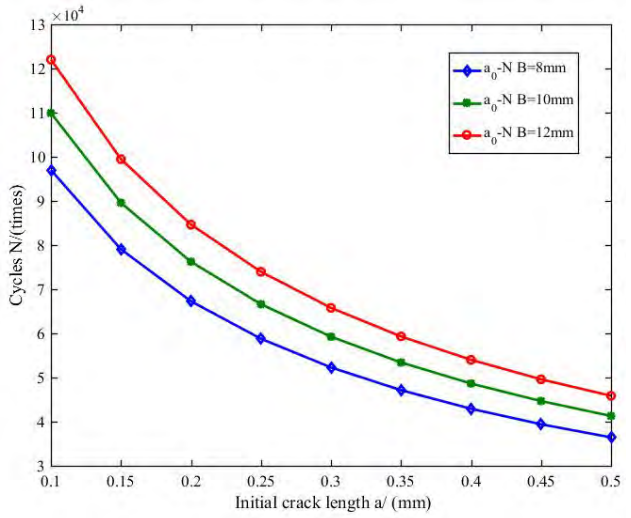

FIGURE 11. Effect of initial crack length on crack propagation life.

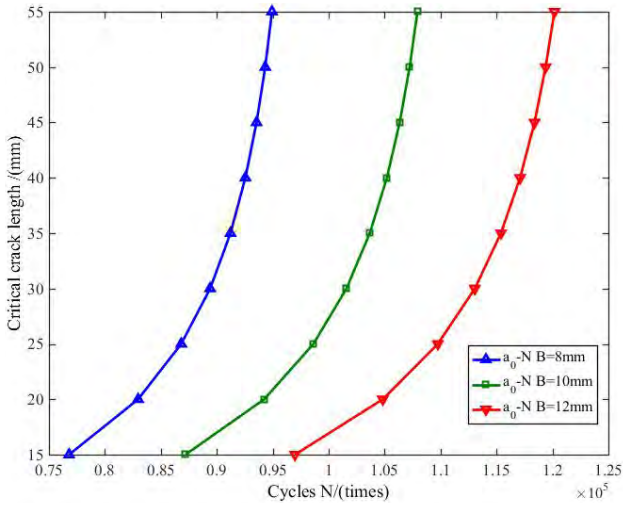

FIGURE 12. Effect of critical crack length on crack propagation life.

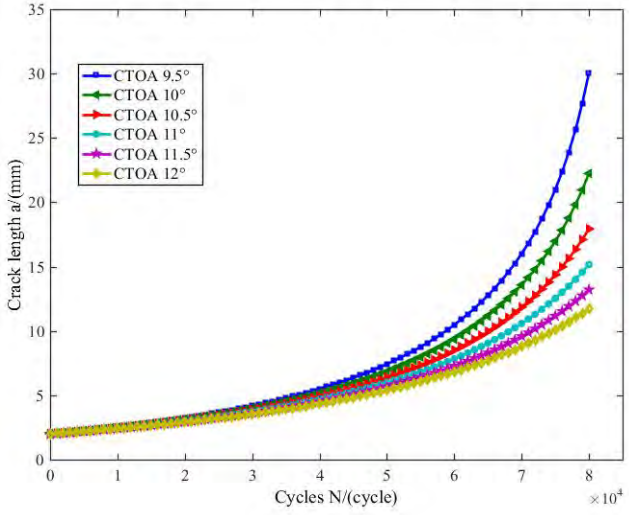

FIGURE 13. Effect of crack opening angle on crack propagation.

thicknesses of 8, 10, and 12 mm were 0.5 mm, the corresponding numbers of cycles are shown in Fig 11 below.

As can be seen from Fig 11, the initial crack length had a significant influence on the fatigue crack growth life. With the same loading conditions, structure, and materials, a smaller initial crack length resulted in greater fatigue crack growth life. With the increase of the initial crack, the crack propagation increased, and the initial crack length and number of cycles were approximately quadratic. When the initial crack length increased from 0.1 to 0.5 mm, the number of cycles was reduced by about 60%. When the initial crack was close to 0.5 mm, the crack propagation life was greatly reduced.

(2) Impact analysis of critical crack parameters

The critical crack length is an important index to determine the instability and expansion of cracks. Determining critical crack lengths is necessary for lifetime predictions of fatigue crack growth. The prediction based on the time-integral crack propagation model for the number of cycles corresponding to different critical crack sizes is shown in Fig 12.

It can be seen from the above Fig 12 that with the same loading conditions, structural form, and materials, the fatigue crack growth lifetimes of the three samples with different thicknesses increased by less than 5% for each 5 mm increase of the critical crack length. As the number of cycles increased, the increase in the number of cycles caused by the increase of cracks gradually decreased. Therefore, the selection of critical cracks has little effect on fatigue life.

(3) Impact analysis of crack tip opening angle parameters

Under the same constant load fatigue test conditions, based on the time integral crack propagation model, the crack propagation curves under different crack opening angles were predicted, as shown in Fig 13.

It can be seen from Fig 13 that the crack opening angle had a greater influence on the crack propagation. When the crack tip opening angle (CTOA) increased from 9.5° to 12°, the crack propagation error was within 1 mm in the initial 40,000 cycles of crack propagation. After 80,000 cycles, the crack propagation length was reduced from 30.05 to 11.75 mm, and the fatigue crack growth life was nearly three times greater. However, as the crack opening angle increased, the influence of the crack opening angle on the crack propagation decreased when the crack opening angle was larger than 10.5°. The lifetime error caused by the 0.5° crack opening angle error was less than 1 mm at 80,000 cycles.

Material CTOA testing is required prior to the crack propagation prediction. Only when the exact crack opening angle is obtained can the fatigue crack propagation life be accurately calculated.

V. CONCLUSION

The crack growth tests of Q345D compact tension specimens with different thicknesses under variable amplitude loading were performed. The lengths of crack propagation and the

numbers of loading cycles were recorded, and the fatigue crack propagation life of the compact tensile specimens were predicted by time integral crack propagation theory. The fatigue test results were in good agreement with the theoretically predicted lifetimes in the first 60,000 cycles, while the maximum error was 10.6% after the 90,000 cycles. This validates the time integration crack propagation theory model. In addition, based on the compact fatigue specimens, the effects of crack opening angle, initial crack length, and critical crack on crack growth were investigated using the time-integral crack growth model. The results show that the initial crack length has a great influence on the fatigue life, and the relationship between them is approximately quadratic. The effect of the crack tip opening angle on the prediction of crack growth life cannot be ignored. When the crack opening angle is greater than 11°, the effect of the crack opening angle decreases significantly. The critical crack had little effect on the fatigue crack growth life. When the fatigue crack propagation reached 30 mm, the fatigue crack propagation life increased by only 5% for every 5 mm increase of the critical crack with unchanged loading conditions, structural form, and material. Comparing it to the traditional fracture mechanics model, the accuracy of the time integral crack growth model was verified. This work provides a reference for the selection of a practical crack growth life prediction model. From the above research, we can clearly see that the plate thickness has a great influence on crack propagation for Q345D. This can guide us to design parts with plate structure. However, many machine structures are not simple plate, they have complex structures. At this time, the crack propagation model of the simple plate cannot reflect the crack propagation in the complex structure. Therefore, it is very necessary to establish a growth model of cracks in complex structures.

REFERENCES

[1] U. Zerbst *et al.*, "Review on fracture and crack propagation in weldments—A fracture mechanics perspective," *Eng. Fract. Mech.*, vol. 132, pp. 200–276, Dec. 2014.
[2] A. J. McEvily, Jr., and R. Boettner, "On fatigue crack propagation in F.C.C. metals," *Acta Metallurgica*, vol. 11, no. 7, pp. 725–743, Jul. 1963.
[3] N. Walker and C. J. Beevers, "A fatigue crack closure mechanism in titanium," *Fatigue Fract. Eng. Mater. Struct.*, vol. 1, no. 1, pp. 135–148, Jan. 1979.
[4] R. G. Forman, V. E. Kearney, and R. M. Engle, "Numerical analysis of crack propagation in cyclic-loaded structures," *J. Basic Eng.*, vol. 89, no. 3, pp. 459–463, Sep. 1967.
[5] J. Newman, "A crack-closure model for predicting fatigue crack growth under aircraft spectrum loading," in *Methods and Models for Predicting Fatigue Crack Growth Under Random Loading*. West Conshohocken, PA, USA, ASTM, 1981.
[6] W. Elber, "The significance of fatigue crack closure," in *Damage tolerance in aircraft structures*. West Conshohocken, PA, USA: ASTM, 1971.
[7] J. R. Mohanty, B. B. Verma, and P. K. Ray, "Prediction of fatigue crack growth and residual life using an exponential model: Part I (constant amplitude loading)," *Int. J. Fatigue*, vol. 31, no. 3, pp. 418–424, Mar. 2009.
[8] J. R. Mohanty, B. B. Verma, and P. K. Ray, "Prediction of fatigue crack growth and residual life using an exponential model: Part II (mode-I overload induced retardation)," *Int. J. Fatigue*, vol. 31, no. 3, pp. 425–432, Mar. 2009.
[9] R. Jones, L. Molent, and K. Walker, "Fatigue crack growth in a diverse range of materials," *Int. J. Fatigue*, vol. 40, pp. 43–50, Jul. 2012.
[10] Z. Lu and Y. Liu, "Small time scale fatigue crack growth analysis," *Int. J. Fatigue*, vol. 32, no. 8, pp. 1306–1321, Aug. 2010.
[11] F. Chen, F. Wang, and W. Cui, "Fatigue life prediction of engineering structures subjected to variable amplitude loading using the improved crack growth rate model," *Fatigue Fract. Eng. Mater. Struct.*, vol. 35, no. 3, pp. 278–290, Mar. 2012.
[12] K. Shi, L. Cai, and C. Bao, "Various Theoretical Models Study of Prediction Fatigue Crack Growth," *J. Mech. Eng.*, vol. 50, no. 18, pp. 50–58, 2014.
[13] C. Bao, L. Cai, and K. Shi, "Prediction of fatigue crack growth rate for small-sized CIET specimens based on low cycle fatigue properties," *Chin. J. Aeronaut.*, vol. 31, no. 4, pp. 740–748, Apr. 2018.
[14] J. A. F. O. Correia, S. Blasón, A. M. P. De Jesus, A. F. Canteli, P. M. G. P. Moreira, and P. J. Tavares, "Fatigue life prediction based on an equivalent initial flaw size approach and a new normalized fatigue crack growth model," *Eng. Failure Anal.*, vol. 69, pp. 15–28, Nov. 2016.
[15] G. R. Irwin, "Analysis of stresses and strains near the end of a crack traversing a plate," *J. Appl. Mech.-Trans. ASME*, vol. E24, pp. 351–369, 1957.
[16] J. Newman, J. Crews, C. Bigelow, and D. Dawicke, "Variations of a global constraint factor in cracked bodies under tension and bending loads," in *Constraint Effects in Fracture Theory and Applications*. West Conshohocken, PA, USA: ASTM, 1995.
[17] J. C. Newman, Jr., C. A. Bigelow, and K. N. Shivakumar, "Three-dimensional elastic-plastic finite-element analyses of constraint variations in cracked bodies," *Eng. Fract. Mech.*, vol. 46, no. 1, pp. 1–13, Sep. 1993.
[18] J. Newman, "Prediction of fatigue crack growth under variable-amplitude and spectrum loading using a closure model,"in *Design of Fatigue and Fracture Resistant Structures*. West Conshohocken, PA, USA: ASTM, 1982.
[19] J. J. Schubbe, "Plate thickness variation effects on crack growth rates in 7050-t7451 alloy thick plate," *J. Mater. Eng. Perform.*, vol. 20, no. 1, pp. 147–154, Feb. 2011.
[20] J. Huo, D. Zhu, N. Hou, W. Sun, and J. Dong, "Application of a small-timescale fatigue, crack-growth model to the plane stress/strain transition in predicting the lifetime of a tunnel-boring-machine cutter head," *Eng. Failure Anal.*, vol. 71, pp. 11–30, Jan. 2017.
[21] W. Sun, J. Ling, J. Huo, L. Guo, and X. Song, "Study of TBM cutterhead fatigue damage mechanisms based on a segmented comprehensive failure criterion," *Eng. Failure Anal.*, vol. 58, pp. 64–82, Dec. 2015.
[22] W. Sun, Y. Zhu, J.-Z. Huo, and X.-H. Chen, "Multiple cracks failure rule for TBM cutterhead based on three-dimensional crack propagation calculation," *Eng. Failure Anal.*, vol. 93, pp. 224–240, Nov. 2018.
[23] P. Yu, C. She, and W. Guo, "Equivalent thickness conception for corner cracks," *Int. J. Solids Struct.*, vol. 47, no. 16, pp. 2123–2130, Aug. 2010.
[24] Y.-B. Shang, H.-J. Shi, Z.-X. Wang, and G.-D. Zhang, "A crack tip driving force model for mode I crack propagation along linear strength gradient: Comparison with the sharp strength gradient case," *Acta Mechanica*, vol. 227, no. 9, pp. 2683–2702, Sep. 2016.
[25] X. Hu *et al.*, "A new cohesive crack tip symplectic analytical singular element involving plastic zone length for fatigue crack growth prediction under variable amplitude cyclic loading," *Eur. J. Mech.-A/Solids*, vol. 65, pp. 79–90, Sep./Oct. 2017.
[26] P. Yu and W. Guo, "An equivalent thickness conception for prediction of surface fatigue crack growth life and shape evolution," *Eng. Fract. Mech.*, vol. 93, pp. 65–74, Oct. 2012.
[27] P. Yu and W. Guo, "An equivalent thickness conception for evaluation of corner and surface fatigue crack closure," *Eng. Fract. Mech.*, vol. 99, pp. 202–213, Feb. 2013.
[28] M. Xiang and W. Guo, "Formulation of the stress fields in power law solids ahead of three-dimensional tensile cracks," *Int. J. Solids Struct.*, vol. 50, nos. 20–21, pp. 3067–3088, Oct. 2013.
[29] W. Guo, Z. Chen, and C. She, "Universal characterization of three-dimensional creeping crack-front stress fields," *Int. J. Solids Struct.*, vols. 152–153, pp. 104–117, Nov. 2018.
[30] Y. Liu, Z. Lu, and J. Xu, "A simple analytical crack tip opening displacement approximation under random variable loadings," *Int. J. Fract.*, vol. 173, no. 2, pp. 189–201, Feb. 2012.
[31] J. Schijve, "Some formulas for the crack opening stress level," *Eng. Fract. Mech.*, vol. 14, no. 3, pp. 461–465, 1981.
[32] G. R. Irwin, "Linear fracture mechanics, fracture transition, and fracture control," *Eng. Fract. Mech.*, vol. 1, no. 2, pp. 241–257, Aug. 1968.
[33] R. C. McClung, "Crack closure and plastic zone sizes in fatigue," *Fatigue Fract. Eng. Mater. Struct.*, vol. 14, no. 4, pp. 455–468, Apr. 1991.

JUNZHOU HUO was born in Yuncheng, Shanxi, China, in 1979. He received the bachelor's degree in mechanical design and theory from the Luoyang Institute of Technology, in 2001, and the Ph.D. degree in mechanical design and theory from the Dalian University of Technology, in 2009.

From 2008 to 2010, he held a postdoctoral position with the School of Naval Architecture, Dalian University of Technology. Since 2013, he has been an Assistant Professor with the Mechanical Engineering Department, Dalian University of Technology, where he has been a Professor, since 2018. He has authored three books, more than 80 articles, and more than 30 inventions. His current research interests include performance optimization of complex mechanical systems, life prediction of main bearing structure, the design of full-face hard rock tunnel boring machine systems.

Dr. Huo is a thousand-level talent in Liaoning, an Outstanding Talent in Higher Education in Liaoning, and an Expert in online evaluation of the National Natural Science Foundation of China. He received the First Prize of the Liaoning Natural Science Excellent Papers, in 2016, the First Prize of the China Construction Management Enterprise Association, in 2017, the Second Prize of the Liaoning Science and Technology Progress Award, in 2017, and the First Prize of the China Machinery Industry Federation, in 2018.

ZHANGE ZHANG was born in Yuncheng, Shanxi, China, in 1990. He received the bachelor's degree in mechanical design and theory from Yuncheng University, Yuncheng, China, in 2012, and the master's degree in mechanical design and theory from Dalian University, Dalian, Liaoning, China, in 2016. He is currently pursuing the Ph.D. degree in mechanical engineering with the Dalian University of Technology, Dalian.

His research interests include the vibration control of complex mechanisms and fatigue damage analysis of complex structures.

Dr. Zhang awards and honors include a national scholarship, in 2015.

ZHICHAO MENG received the B.S. degree in mechanical engineering from the Taiyuan University of Technology, Taiyuan, China, in 2016. He is currently pursuing the Ph.D. degree in mechanical engineering from the Dalian University of Technology, Dalian, China.

His Ph.D. research topics are visual recognition technology of wear state of TBM hobs. His research interests include remote monitoring of TBM health status, including real-time monitoring of TBM host vibration status, and stress and strain measurement of TBM cutter head.

LIN XUE received the bachelor's and master's degrees in mechanical engineering from the Dalian University of Technology, Dalian, Liaoning, China, and the Ph.D. degree from The University of Tokyo, Tokyo, Japan. He is currently a master's supervisor with the Dalian University of Technology.

His research interests include high precision industrial CT and nondestructive testing, machine vision, and industrial 2D 3D image processing.

GUOPENG JIA received the B.S. and M.S. degrees in mechanical engineering from the Shandong University of Technology, Zibo, Shandong, China, in 2015 and 2018, respectively. He is currently pursuing the Ph.D. degree in mechanical engineering with the Dalian University of Technology, Dalian, Liaoning, China. His research interest includes big data analysis of TBM, performance optimum design of mechanisms, and machine learning using in mechanical field.

JING CHEN received the bachelor's degree in mechanical design and theory from the Luoyang Institute of Technology, in 2000, and the M.S. and Ph.D. degrees in design and manufacture of ships and ocean engineering structures from the Dalian University of Technology, in 2011.

Since 2014, she has been an Assistant Professor with the College of Navigation and Shipbuilding Engineering, Dalian Ocean University. She has authored one book and more than 15 articles. Her current research interests include intelligent optimum design of ship master scheme and optimum design method of ship ballast water replacement.